Paper No. 236—1

Distribution of Corrosion Fatigue Crack Lengths in Carbon Steel*

(1st Report, The Cracks which Grow Individually)

By Sotomi ISHIHARA**, Kazuaki SHIOZAWA*** and Kazyu MIYAO****

It has been known that very small distributed cracks can be observed on the surface of a smooth specimen subjected to corrosion fatigue. The fracture process can be characterized by the interaction and coalescence of these small distributed cracks. In order to analize this corrosion fatigue fracture process, high cycle fatigue tests were performed on carbon steel sheet specimens under completely reversed plane bending stresses in salt water(3.0%NaCl).

Initiation and growth of cracks on the surface of smooth specimen were observed in detail during corrosion fatigue process. The distribution of crack lengths at a certain stress cycles was able to be explained by a statistical calculation which took into account both the variation of number of cracks during stress cycling and the scatter of crack growth rates.

Key Words : Corrosion Fatigue, Carbon Steel, Distribution of Crack Lengths, Crack Initiation

1. Introduction

Many small distributed cracks have been often observed at the surface of unnotched specimens subjected to corrosion fatigue, thermal fatigue, low-cycle fatigue and fretting corrosion fatigue. This fracture process can be characterized by two stages, that is,the crack initiation, crack growth during which cracks interact and coalesce. From the viewpoint of strength design of machine and structures and safety maintenance of them, it may be important to have full understanding of this fracture process.

The authors have studied the effects of tensile prestrain on corrosion fatigue strength of smooth specimens of aluminum alloy [1-3] and carbon steel [4] , and pointed out that the quantitative analysis is necessary to evaluate the initiation and growth behaviour of distributed fatigue cracks caused by corrosion fatigue, and the corrosion fatigue lives of smooth specimens. However,there are a few studies [3][5-7] concerning the behaviours of distributed cracks during fatigue process. This may be because the initiation and growth behaviours of the distributed fatigue cracks are probabilistic, therefore, these distributed cracks is difficult to analyze qualitatively without statistical evaluation of them.

Kitagawa *et al.* [5][6] are the pioneers in the studies which treat the problem of the distributed cracks. They explained the corrosion fatigue process considering the behaviours of initiation, its spatial distribution, interaction and coalescence of distributed cracks using Monte-carlo method and displayed on graphic display. Tanaka *et al.* [9] reported that the distribution of crack lengths after a certain number of stress cycles initiated from a few randomly distributed defects can be derived analytically. Tokaji *et al.* [7] experimented and investigated the difference of the distribution of crack lengths observed on the specimen surface during the fatigue process of carbon steel in laboratory air,water and salt water respectively, and reported that the distribution of crack lengths is represented as a Weibull distribution.

The authors discribe in this paper the estimation method of fatigue life where numerous cracks are initiated, theoretical analysis of the distribution of crack lengths after a certain number of stress cycles.

Plane bending fatigue tests were performed using smooth specimens of carbon steel in salt water (3%NaCl), and the initiation and growth behaviours of distributed cracks on the smooth specimen surface were investigated in detail by successive observation of its surface during fatigue process. Two types of cracks were observed : One (designated as F_1) propagates as a single crack without interaction with the others; The other(designated as F_2) propagates with the interaction and coalescence of closely located surface cracks. From the authors' experimental results, the method to estimate the former (F_1) type of distributed cracks can be derived theoretically by considering both the initiation and growth behaviours of the distributed cracks. The quantitative analysis of the latter type of cracks(F_2)will be described in the authors following report.

* Received 5th Nov., 1982.

** Assistant, Faculty of Engineering, Toyama University,Toyama 930,Japan.
*** Associate Professor,Faculty of Engineering,Toyama University,Toyama 930 , Japan.
**** Professor, Faculty of Engineering, Toyama University,Toyama 930,Japan.

2. Main Symbols

2ℓ : Crack length (ℓ : half crack length)
F_1 : Cracks which propagate as a single crack without interaction with others.
F_2 : Cracks which show the interaction and coalescence of closely located surface cracks.
F : $F = p_1F_1 + p_2F_2$
p_1 : The probability of existence for F_1.
p_2 : The probability of existence for F_2.
N : Number of stress cycles.
N_f : Number of stress cycles to failure.
N_c : Number of stress cycles to the earliest crack initiation.
n : Number of cracks per unit area.
n_0 : Saturated number of cracks per unit area.
β : Crack initiation rate.
σ : Stress amplitude.
ΔK : Stress intensity factor range.
C, m : The constants in the Paris-equation, $d\ell/dN = C\Delta K^m$.
C' : The constant in the crack growth equation for F_2, $d\ell/dN = C'$.
k : $k = \log C$
N_0 : Number of stress cycles to appearance of cracks.
ℓ_0 : Half crack length when cracks appear.
$\bar{m}$: The mean value of m.
$\bar{k}$: The mean value of k.
S_k : Standard deviation of k.

3. Material and Experimental Procedures

The material tested was a low-carbon steel, JIS SS41, whose chemical composition and mechanical properties are listed in Table 1 and Table 2, respectively. The latter was obtained after annealing treatment. Shape and dimension of the specimen are shown in Fig. 1. Flat specimens were machined from a 3 mm thick rolled plate. Longitudinal direction of the specimen was taken in rolled direction. After mechanical polishing with emery-paper(#1000), specimens were annealed at 1173K for one hour in vacuum. The ferrite grain size was examined about 52μm in diameter. Specimen was tested by fatigue testing machine after electropolishing by 30 μm. The surface of the specimen was coated with silicone rubber except for a central area of 16 by 16 mm as shown in Fig. 1 on which region the cracks were observed.

Table 1 Chemical composition of the material

C	Si	Mn	P	S
0.16	0.01	0.42	0.019	0.02

Table 2 Mechanical properties of the specimen

Yield strength σ_y MPa	Tensile strength σ_B MPa	Elongation ϵ_f %
175	328	71.1

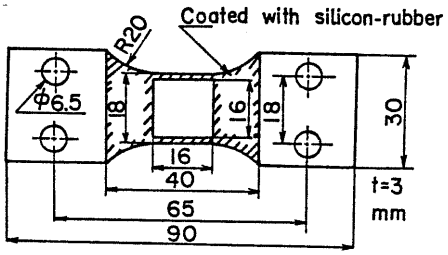

Fig. 1 Shape and dimension of the specimen

The specimen surface was observed successively by the Replica method as follows: Fatigue test was stopped after an appropriate number of stress cycles, and cracks were replicated on replica film from the specimen surface. Cracks were examined on the replica film enlarged to 30~40 times. Fig. 2 is an example of the photo which shows the morphology of the distributed cracks on the specimen surface fatigued in salt water at σ=127MPa. From this figure, crack length of 20 μm could be measured at least.

The difference between fatigue life under successive corrosion fatigue test and that of intermittent one is little (±20%), and so, the effects of elimination of corrosion products on corrosion fatigue behaviours are considered to be small.

Fatigue tests were carried out using a Schenk-type bending machine whose cyclic speed was 60 Hz, and completely reversed plane bending was done. The environment in the present tests was salt water (3%NaCl) kept at 298± 0.5K, which was dripped at a rate of 20~30 ml per minute on the specimen surface. If specimen's stiffness was decreased during fatigue, loading condition was adjusted so as to secure constant bending moment tests. Experimental details are reported elsewhere [1], so omitted in this paper. S-N curves obtained in these experiments are shown in Fig. 3.

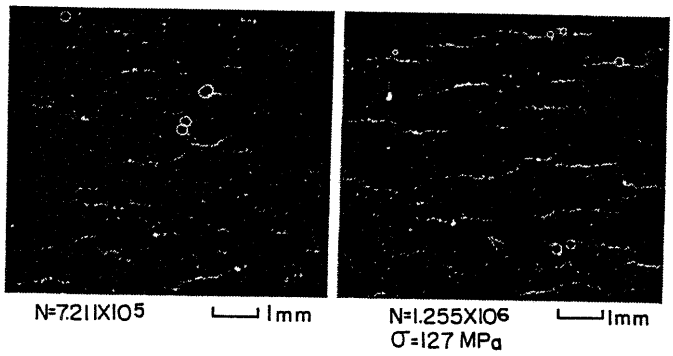

Fig. 2 Appearances of the distributed cracks initiated on the specimen surface during corrosion fatigue

4. Experimental Results and Discussion

4.1 The initiation behaviours of the distributed cracks

The relations between number of cracks per unit area, n, and stress cycles, N, in corrosion fatigue are shown in Fig. 4 for the cases of 98, 127 and 147 MPa. As seen from this figure, cracks are initiated in the early stage of corrosion fatigue and in this stage, the increase rate of number of cracks per unit area with stress cycles is large, but thereafter, it tends to saturate and settle to a constant value. Therefore, the relations between n and number of stress cycles, N, are approximated by the following equation;

$$\left.\begin{aligned} n &= n_0\{1-e^{-\beta(N-N_c)}\} \\ N &\geqq N_c \end{aligned}\right\} \quad \cdots\cdots\cdots (1)$$

where, N_c in the above equation is the number of cycles to the earliest crack initiation. In corrosion fatigue, N_c may be nearly equal to zero. Experimentally obtained values of n_0 and β are shown in these figures. Crack density decreases slightly in the latter stage of fatigue of 127 and 147 MPa. For this reason, it may be thought that the decrease in crack density which comes from regarding connected cracks as a single one exceeds the increase in crack density which comes from initiation of new cracks. Therefore, in approximating n-N relation as Eq. (1), we must pay attention to the effective range of its approximations.

Next, the relation between n_0, β and stress amplitude σ is given in Fig.5. From this figure, it can be seen that linear relationships between $\ln n_0$, $\ln\beta$ and σ are established experimentally, and they may be treated as a rate process governed by stress amplitude.

$$\left.\begin{aligned} \beta &= C_1 \exp(C_2\sigma) \\ n_0 &= C_3 \exp(C_4\sigma) \end{aligned}\right\} \quad \cdots\cdots\cdots (2)$$

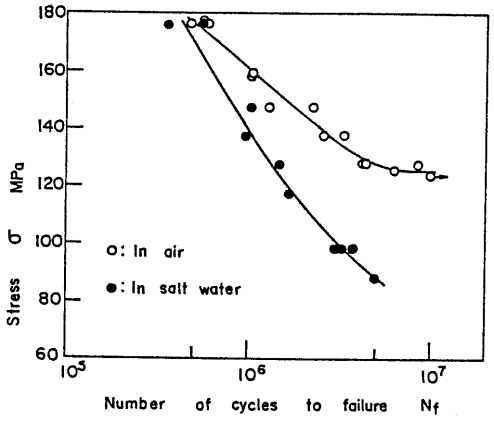

Fig. 3 S - N diagram

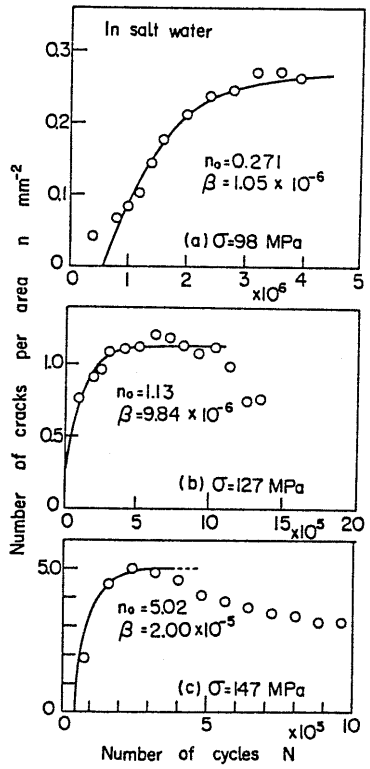

Fig. 4 Change of number of cracks per mm^2 during stress cycling in salt water

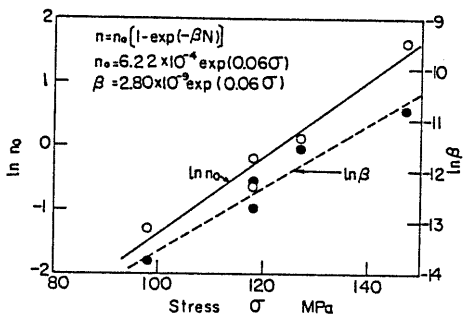

Fig. 5 Relation between n_0, β and stress amplitude

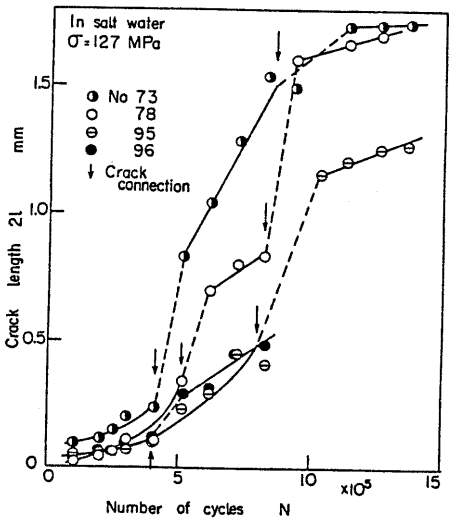

Fig. 6 Examples of crack growth curves in salt water at σ = 127 MPa

Experimentally obtained relationships are given in Fig. 5. The constants, C_1, C_2, C_3 and C_4 in Eq. (2) are independent of stress amplitude, but may be affected by various environmental, metallurgical and mechanical factors, and perhaps a further detailed study may be necessary.

4. 2 The behaviour of crack growth

Examples of crack growth curves obtained by successive observation of smooth specimen surface under corrosion fatigue are shown in Fig. 6. Though the initiation time for each crack differs from case to case, crack growth curves are plotted for convenience as if all of the cracks were initiated at the same time of N=0. As seen from this figure, there are two types of crack growth behaviours. That is, one propagates as a single crack without interaction with others, and the other shows the interaction and coalescence of closely located surface cracks. The latter is a discontinuous growth behaviour which gives staircase-like growth curves. In an other study[10], crack growth rate was obtained by approximating discontinuous growth curves shown in Fig. 6 with smoothed curves, while in the present study, crack growth rate is discussed by separating crack growth behaviour before crack coalescence from that after crack coalescence.

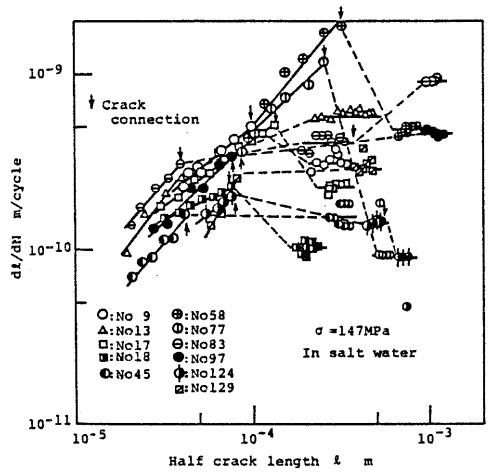

Fig. 7 Change in crack growth behaviours before and after crack coalescence

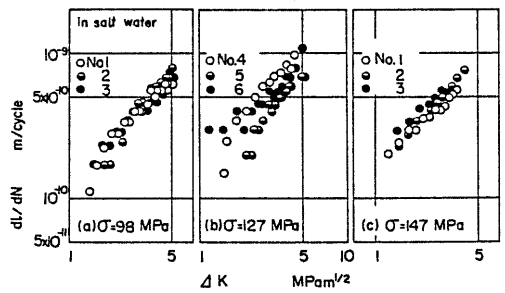

Fig. 8 Relation between crack growth rate ($d\ell/dN$) and stress intensity factor range (ΔK) for cracks which grow as a single crack

The relation between crack growth rate, $d\ell/dN$ and half crack length, ℓ, is shown in Fig. 7. As an example, the results of σ = 147MPa are given. As seen from this figure, it is obvious that $d\ell/dN$ before crack coalescence is dependent on ℓ, but $d\ell/dN$ after crack coalescence is not dependent on ℓ. The relation between crack growth rate, $d\ell/dN$, and stress intensity factor range, ΔK, is given in Fig. 8 for the crack which propagates as a single crack. As examples, the results of 98, 127 and 147MPa are shown. ΔK is defined as follows;

$$\Delta K = \sigma\sqrt{\pi l} \quad \cdots\cdots(3)$$

It can be seen from this figure that there exist linear relationships between $\log(d\ell/dN)$ and $\log(\Delta K)$, and therefore, the following Paris-equation is derived.

$$dl/dN = C\Delta K^m \cdots\cdots(4)$$

For each crack, C and m in Eq. (4) were decided by using the least square method excluding the experimental points which obviously deviate from the regression line between $d\ell/dN$ and ΔK. The values of C and m for each crack are different. So, the values of logC and m were plotted on a normal probability paper. The results are shown in Fig. 9 for the cases of 98, 127 and 147 MPa. The ordinate indicates the cumulative probability of k(=logC) and m, and is represented by $t_i/(t_0+1)$, where t_i is the rank obtained by arranging the values of k and m according to their size, and t_0 is the number of samples.

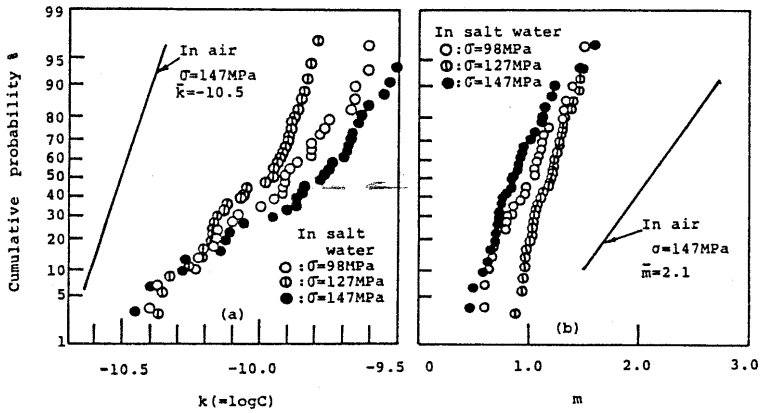

Fig. 9 The distribution of the constants C and m (normal probability paper)

It can be seen from Fig. 9 that the statistical distributions of C and m are logarithmic normal and normal respectively. The values of $\bar{k}$, S_k, $\bar{m}$ and S_m for each stress amplitude are shown in Table 3. From Fig. 9 and Table 3, it may be seen that the values of $\bar{m}$, $\bar{k}$, S_k and S_m are nearly independent of stress amplitude and regarded to be constant. The average value of m, $\bar{m}$, is about 1.02, which is considered to be smaller than that obtained usually for a single through crack. The distributions of m and k obtained from fatigue tests conducted at σ=147 MPa in laboratory air using the same specimens as the ones of this study are also plotted in Fig. 9. In this case, the values of $\bar{m}$ is 2.1. This discrepancy between the two values of $\bar{m}$ mentioned above may be due to the following reasons: In corrosion fatigue, most of cracks are initiated from corrosion pits, therefore, the small crack growth behaviours may be affected by these corrosion pits and the variance of crack aspect ratio with crack length. Furthermore, in corrosion fatigue, the degree of dependence of crack growth rate on stress intensities is lowered by stress relaxation and crack interaction which may be due to the initiation of many cracks during fatigue at each of crack tips. At present, it is not obvious what is the most important factor among them, so a more detailed study may be necessary.

Kitagawa *et al.* [11] reported that the following relation between C and m in the Paris-equation had been established:

$$C = AB^m \quad \cdots\cdots\cdots\cdots (5)$$

Table 3 Values of the parameters

Stress MPa	$\bar{m}$	Sm	$\bar{k}$	Sk
98	1.01	0.30	-9.94	0.26
127	1.17	0.18	-9.97	0.18
147	0.88	0.24	-9.91	0.24
Average	1.02	0.24	-9.94	0.23

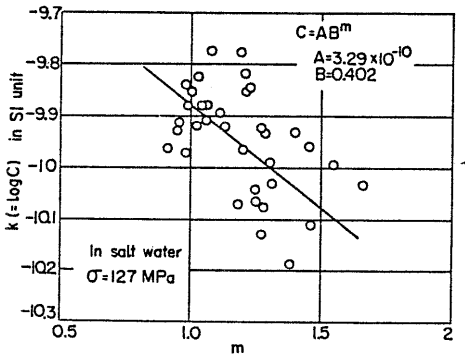

Fig. 10 Correlation between C and m

About the crack growth behaviours of the distributed surface cracks under corrosive environment in the present study, it was examined whether Eq. (5) can hold or not. For the case of σ=127 MPa, the result of this examination is given in Fig. 10. From this figure, though experimental data locate over a somewhat wide range, it can be seen that a linear relationship holds between logC and logm, and Eq. (5) is nearly established. Experimentally obtained equation between C and m is shown in this figure.

When a crack which grows following the Paris-equation connects with another crack, the connected cracks grow as a single crack and their growth rate under constant stress amplitude is approximated by the following equation, as seen from Fig. 7:

$$dl/dN = C' \quad \cdots\cdots\cdots\cdots (6)$$

For this reason, the following are likely: If two of semi-elliptical surface cracks interact and connect with each other, the three-dimensional shape of the connected cracks immediately after crack connection will be a half guitar-shaped one.
Stress intensity factor at both ends of the surface crack having the shape just mentioned is smaller [12] than that of a semi-elliptical surface crack under the condition that their crack lengths at surface are equivalent. Therefore, a decrease in crack growth rate may be observed immediately after crack connection if crack growth rate is measured only by surface crack length.
As crack shape like a half guitar immediately after crack connection changes into a semi-elliptical crack shape, it is expected that the crack growth behaviours represented by Eq. (6) change steadily to the one in which crack growth rate depends on crack length (the Paris-equation represented by Eq. (4)). However, in this experiment, the distributed cracks initiated on the specimen surface are so many that the probability of interaction and connection of these cracks becomes high, and therefore, the cracks immediately after crack connection connect

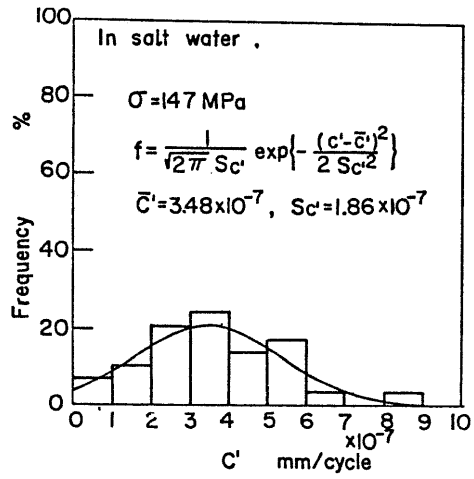

Fig. 11 Distribution of C' appearing in crack growth law for crack group F_2, $d\ell/dN = C'$

with other surrounding cracks successively before a guitar-shaped crack recovers the semi-elliptical shape. This may be the reason why the decrease in crack growth rate after crack connection is observed successively as shown in Fig. 7. As another reason why Eq. (6) is obtained, it may be considered that the crack immediately after crack connection cannot recover the semi-elliptical shape when the stress relaxation occurs at a place where many cracks are initiated.

The values of C' in Eq. (6) are different from each other depending on the combination of single crack which have various crack lengths and crack shapes. A histogram of C' is shown in Fig. 11 for the case of σ=147 MPa. The solid line in this figure indicates the best fit of the experimental distribution of C' approximated by a normal distribution. From this figure, it may be considered that the distribution of C' is a normal one.

4. 3 The distribution of crack lengths

From the photograph of the distributed cracks shown in Fig. 2 and crack growth behaviours stated in section 4.2, cracks are classfied into two types. That is, one(designated F_1) propagates as a single crack and the other (designated F_2) shows the interaction and coalescence of closely located surface cracks. When cracks are apart from one another, it is likely that the interaction between them is little and the growth rate obeys the Paris-equation. However, when cracks approach one another, the degree of the interaction between them increases and the crack growth behaviours change from one in which crack growth rate obeys the Paris-equation to one in which crack growth rate is constant independently of number of stress cycles. At this moment, it is supposed in this study that the crack which belongs to F_1 changes the one which belongs to F_2 and that interacting cracks coalesce and form a new single crack.

When stress amplitude is high, two interacting cracks whose growth rates follow Eq. (6) coalesce with one another easily, but when stress amplitude is low, crack tips of two interacting cracks cannot coalesce with each other and this interacting condition continues for long period. For this reason, though two cracks coalesce with one another actually within the specimen, it seems that the remaining parts of the materials between two interacting cracks are not broken easily, when stress amplitude is low and stress relaxation occurs at the place of crack coalescence.

Using the photographs of the replica taken at a certain number of stress cycles, the number of cracks for a certain range of crack lengths was investigated and the result is shown in Fig. 12 taking the cumulative probability as ordinate and crack length, 2ℓ, as abscissa. The results of 98 and 147 MPa are given as examples. The experimental data points represented by ◑, ● and ○ in the figure correspond to the crack groups F_1, F_2 and F respectively, where crack group F shows the distribution of crack lengths for all of the cracks without classification of cracks into F_1 and F_2.

As for the effects of the magnitude of stress amplitude on the distribution of crack lengths, in the high stress amplitude (147 MPa), there are many cracks which belong to crack group F_2, and both the cracks which belong to F_1 and the cracks which belong to F_2 exist at the same time for a certain range of crack lengths. Therefore, the crack group F is represented by the following mixed type distribution of F_1 and F_2:

$$\left.\begin{aligned} F(2l) &= p_1F_1(2l)+p_2F_2(2l) \\ p_1+p_2 &= 1 \end{aligned}\right\} \quad \cdots\cdots\cdots\cdots (7)$$

where, p_1 and p_2 represent the probability of existence for F_1 and F_2, respectively. On the other hand, in the low stress amplitude(98 MPa), most of cracks belong to the crack group F_1. Though the cracks which belong to F_2 are observed in the latter stage of fatigue, even in the case, F tends to show a more compound type distribution of F_1 and F_2 than mixed type distribution.

The variation of p_1 with stress cycling

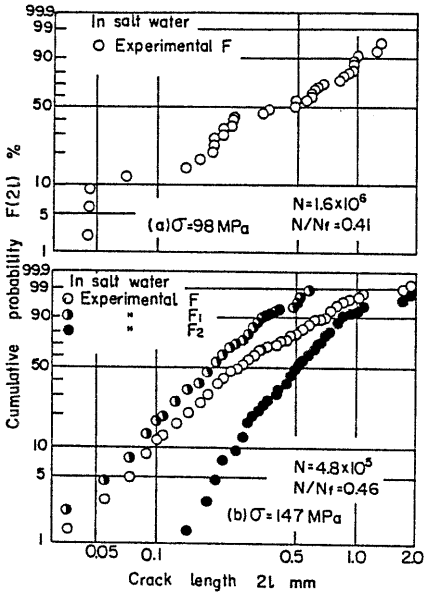

Fig. 12 An example of the distribution of crack lengths obtained experimentally

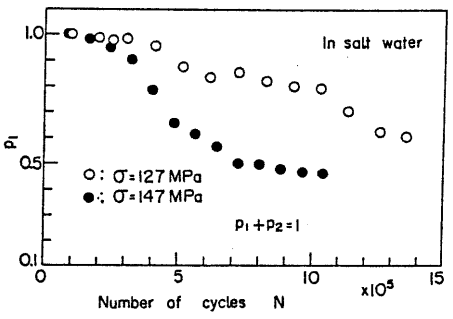

Fig. 13 Change of the crack existence rate p_1 for crack group F_1 with stress cycles in salt water

is shown in Fig. 13 for the case of σ=127 and 147 MPa. As seen from this figure, the values of p_1 decrease monotonously with stress cycles and this trend is independent of stress amplitude, but the degree of this lowering in p_1 for σ=147 MPa is larger than that for σ=127 MPa. Considering $p_1+p_2=1$, p_2 increases with N monotonously.
In this study, it was assumed that one crack is produced when a coalescence of the distributed cracks has occurred.

5. Derivation of the Distribution of Crack Lengths (The crack group F_1 which grows as a single crack)

In this chapter, the distribution of crack lengths during fatigue process will be discussed theoretically considering both the crack initiation and propagation behaviours of the distributed cracks obtained experimentally and stated in the section 4.1 and 4.2. As stated before, two types of cracks whose crack growth behaviours were different from each other were observed during fatigue process, so, in order to derive the distribution of crack lengths theoretically, it will be important to follow the mechanism of crack growth for each crack group faithfully. In this chapter, a quantitative calculation method for the distribution of crack lengths in crack group F_1 is described, and crack group F_2 will be treated in the next study.

Let us consider the Paris-equation represented by Eq. (4) as crack growth law. By integrating Eq. (4) with initial condition that $\ell=\ell_0$ at $N=N_0$, the following equation is obtained;

$$l=\left[l_0^{(2-m)/2}+(\sigma^2\pi)^{m/2}\times\frac{2-m}{2}C(N-N_0)\right]^{2/(2-m)},$$
$$(m\neq 2) \quad \cdots\cdots(8)$$

In above equation, replacing $m_1=(2-m)/2$, Eq. (8) can be written as follows:

$$l^{m_1}-l_0^{m_1}=(\sigma^2\pi)^{1-m_1}\, m_1\, C(N-N_0) \cdots\cdots(9)$$

For the calculation of distribution of crack lengths, it is important to examine whether a correlation between C and m should be considered or not. In the next section, the calculation method of the distribution of crack lengths in which m is taken as constant and C is a probabilistic variable will be described. Then a calculation method of the distribution of crack lengths in which correlation between C and m in Eq. (13) is taken into consideration will be introduced.

5. 1 Case 1 : m is constant and C is a probabilistic variable

In Eq. (9), the variables are replaced as follws: $B_0=m_1(\sigma^2\pi)^{1-m_1}(N-N_0)$, $\log(\ell^{m_1}-\ell_0{}^{m_1})=t$, $\log B_0=b$, $\log C=k$, which leads to the following equation:

$$t=b_0+k \cdots\cdots(10)$$

Here, for the value of m, the average of $\bar{m}$ listed in Table 3 will be employed.
As the distribution of C is logarithmic normal from experimental results shown in Fig. 9, the distribution of k, f(k), is normal, that is,

$$f(k)=\frac{1}{\sqrt{2\pi}S_k}\exp\left\{-\frac{(k-\bar{k})^2}{2S_k^2}\right\} \cdots\cdots(11)$$

where $\bar{k}$ and S_k are the mean value and standard deviation of k, respectively. From Eq. (10), the probabilistic density function for t is found as follows:

$$h(t)=\frac{1}{\sqrt{2\pi}S_t}\exp\left\{-\frac{(t-\bar{t})^2}{2S_t^2}\right\} \cdots\cdots(12)$$

where $\bar{t}$ and S_t are the mean value and standard deviation of t, respectively.
The following relationships hold between $\bar{t}$, S_t and $\bar{k}$, S_k:

$$S_t=S_k,\ \bar{t}=\bar{k}+b_0 \cdots\cdots(13)$$

After the conversion of probabilistic variables, the probabilistic density function for the half crack length, i(ℓ), has the following relationship with h(t):

$$i(l)=h(t)\left|\frac{dt}{dl}\right|=\frac{1}{\sqrt{2\pi}S_k}\times\exp\left[-\frac{\{\log(l^{m_1}-l_0^{m_1})-\bar{k}-b_0\}^2}{2S_k^2}\right]\times\left|\frac{m_1 l^{m_1-1}}{l^{m_1}-l_0^{m_1}}\right| \cdots\cdots(14)$$

Function i(ℓ) is a probabilistic density function for the length of a crack which is initiated at a number of cycles N_0 and observed at a number of cycles N. The relationship between the density of cracks, n, and the number of cycles of loading, N, is approximated as Eqs. (1) and (2) for variable stress amplitude. Therefore, the probability density function $f_1(\ell,\sigma,N)$ for all of the cracks that have been initiated until stress cycles N is given as follows:

$$f_1(l,\sigma,N)=\frac{1}{n}\int_{N_c}^{N} i(l)\frac{dn(N_0,\sigma)}{dN_0}dN_0 \cdots(15)$$

and therefore the distribution function $F_1(\ell,\sigma,N)$ is obtained by integrating Eq.(15):

$$F_1(l,\sigma,N)=\frac{\beta}{\sqrt{2\pi}\{1-e^{-\beta(N-N_c)}\}S_k}\times\int_{l_0}^{l}\int_{N_c}^{N}\exp\left[\left[-\{\log(l^{m_1}-l_0^{m_1})-g-\log(N-N_0)\}^2/2S_k^2\right]-\beta(N_0-N_c)\right]\times\left|\frac{m_1 l^{m_1-1}}{l^{m_1}-l_0^{m_1}}\right|dN_0dl \cdots\cdots(16)$$

where, $g=\bar{k}+\log\{m_1(\sigma^2\pi)^{1-m_1}\}$.

5. 2 Case 2 : Correlation between C and m considered

Taking the common logarithm of both sides of Eq. (5) and using $\log C=k$, $\log A=a$ and $\log B=b$, the following equation is obtained:

$$k=a+mb \cdots\cdots(17)$$

Using Eq. (17), m_1 can be expressed as follows:

$$m_1=(2-m)/2=(2b-k+a)/2b \cdots\cdots(18)$$

Substituting Eq. (18) into Eq. (8), the following equation is obtained:

$$l^{m_1}-l_0^{m_1}=(\sigma^2\pi)^{1-m_1}10^{a+2b(1-m_1)}m_1(N-N_0) \cdots\cdots(19)$$

Assigning $j(\ell)$ and $g(m_1)$ as the probabilistic density functions for half crack length, ℓ and m_1, respectively, the following relationship is obtained:

$$j(l)=g(m_1)\left|\frac{dm_1}{dl}\right| \quad \cdots\cdots(20)$$

As the distribution of k is normal, the probabilistic density function of m_1, $g(m_1)$, is given by the following equation:

$$g(m_1)=\frac{1}{\sqrt{2\pi}S_{m_1}}\exp\left[-\frac{(m_1-\bar{m}_1)^2}{2S_{m_1}^2}\right] \quad \cdots\cdots(21)$$

where, $\bar{m}_1$ and S_{m_1} are the mean value and standard deviation of m_1, respectively. The following relationships hold between $\bar{m}_1$, S_{m_1} and $\bar{k}$, S_k.

$$\bar{m}_1=(2b+a-\bar{k})/2b,\ S_{m_1}=S_k/|2b| \quad \cdots\cdots(22)$$

Next, using Eq. (19), the value of $|dm_1/d\ell|$ can be calculated, and then, substituting this into Eq. (20), a final expression for $j(\ell)$ is obtained as follows:

$$j(l)=\frac{1}{2.3\sqrt{2\pi}S_{m_1}}\exp\left[-\frac{(m_1-\bar{m}_1)^2}{2S_{m_1}^2}\right]\left|\frac{-m_1 l^{m_1-1}}{(l^{m_1}-l_0^{m_1})\{2b+\log(\sigma^2\pi)-\frac{1}{2.3m_1}\}+l^{m_1}\log l-l_0^{m_1}\log l_0}\right| \quad \cdots(23)$$

The variation of the density of cracks, n, with stress cycles of loading is represented by Eqs. (1) and (2) for various stress amplitudes. Therefore, the probabilistic density function $f(\ell,\sigma,N)$ for all of the cracks that have been initiated until stress cycles N is given as

$$f(l,\sigma,N)=\frac{1}{n}\int_{N_c}^{N}j(l)\frac{dn(N_0,\sigma)}{dN_0}dN_0 \quad \cdots\cdots(24)$$

and therefore, the distribution function $F_1'(\ell,\sigma,N)$ is obtained by integrating Eq. (24):

$$F_1'(l,\sigma,N)=\frac{\beta}{2.3\sqrt{2\pi}S_{m_1}\{1-e^{-\beta(N-N_c)}\}}\int_{l_0}^{l}\int_{N_c}^{N}\exp\left[-\frac{(m_1-\bar{m}_1)^2}{2S_{m_1}^2}-\beta(N_0-N_c)\right]$$
$$\times\left|\frac{-m_1 l^{m_1-1}}{(l^{m_1}-l_0^{m_1})\left\{2b+\log(\sigma^2\pi)-\frac{1}{2.3m_1}\right\}+l^{m_1}\log l-l_0^{m_1}\log l_0}\right|dN_0dl \quad \cdots\cdots(25)$$

6. Numerical Results and Discussion

6. 1 Examination about whether correlation between C and m in the Paris-equation should be considered or not

Numerical calculation for the distribution of crack lengths was performed using Eqs. (16) and (22) at σ=127 MPa, and the integrals were evaluated by means of Simpson's rule. An example of these numerical results together with experimental results is shown in Fig. 14. Experimental data correspond to those for the cracks which propagate as a single crack. The distribution of crack lengths calculated without consideration of correlation between C and m is represented by a solid line, and the results calculated with correlation between C and m is represented by a dotted line. The values of the

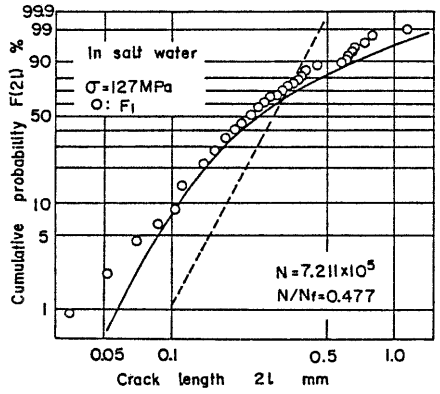

Fig. 14 Investigation about whether correlation between C and m in Paris-equation should be considered or not

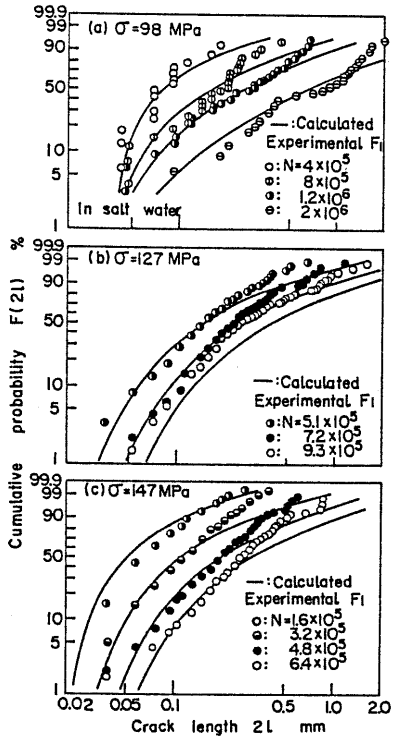

Fig. 15 Comparison between numerical results and experimental results about the distribution of crack lengths F_1

parameters needed for these numerical calculation were obtained from experimental results stated in the sections 4. 1 and 4. 2. It can be seen from this figure that numerical results without consideration of correlation between C and m nearly correspond with experimental results, whereas numerical results with correlation between C and m show a tendency in which crack lengths are distributed over a more restricted region , and they do not correspond with experimental results. This tendency is also reported in the study of Sakai *et al.* [13] in which crack growth period for a single crack initiated from notch was analized. This disagreement with experimental results may be due to postulation that all of the experimental data points fall on the regression line between $d\ell/dN$ and ΔK, and it may be thought that, even if Eq. (5) holds and correlation between C and m is apparent within the limits of experimental data shown in Fig. 10, correlation between C and m observed for enough data from a statistical viewpoint does not always hold [14]. As the other reasons, it may be stated that though the scatter in the value of k for a certain value of m is somewhat large, postulation of Eq. (5) results in ignoring this scatter of k.

As stated above, in calculating the distribution of crack lengths, the experimental results could be explained well by the calculation method in which m was taken as constant and C was a probabilistic variable, as shown in Fig. 14.

6. 2 Comparison between numerical results and experimental results about the distribution of crack lengths

From the examination in section 6.1, substituting experimentally obtained data, $\bar{k}$, S_k, $\bar{m}$ and β in sections 4.1 and 4.2 into Eq. (16), the distribution of crack lengths for a certain number of cycles of loading and stress amplitude can be evaluated numerically, and the results for σ=98, 127 and 147 MPa are shown in Fig. 15 by solid lines. The values of $\bar{m}$, $\bar{k}$ and S_k were considered constant independently of stress amplitude, and the mean values of the experimental data were employed. From this figure, it can be seen that the distribution of crack lengths shifts in the right direction with stress cycling and calculated results for the distribution of crack lengths coincide well with experimentally obtained results.

7. Conclusions

Using smooth specimens of carbon steel, plane bending fatigue tests were conducted in salt water(3%NaCl). And, how the crack initiation and growth behaviours of the distributed cracks correspond to the change in the distribution of crack lengths during fatigue was investigated by means of successive observation of specimen surface, with the following results obtained.

(1) The distribution of crack lengths can be rearranged as a single distribution in the early stage and in the region of low cyclic stress amplitudes of corrosion fatigue, while, in the latter half stage and in the region of high cyclic stress amplitudes of corrosion fatigue, the distribution of crack lengths can be represented by a mixed type distribution which is composed of F_1 which propagates as a single crack and F_2 which shows the interaction and coalescence of closely located surface cracks.

(2) The crack growth behaviours for crack group F_1 are nearly represented by the Paris-equation, $d\ell/dN=C\Delta K^m$. C and m have different values for each crack, and their distributions are logarithmic normal and normal, respectively. The following correlation holds between C and m, $C=AB^m$.

(3) In the Paris-equation, $d\ell/dN=C\Delta K^m$, the mean value of k (k=logC), $\bar{k}$, standard deviation, S_k and the mean value of m, $\bar{m}$, were nearly constant independently of stress amplitude in this experiment.

(4) The change of crack density, n, initiated during corrosion fatigue with stress cycles can be represented by the following equation, $n=n_0\{1-e^{-\beta(N-N_0)}\}$, where n_0 and β are functions of stress amplitude and written as

$\beta=C_1\exp(C_2\sigma)$, $n_0=C_3\exp(C_4\sigma)$.

(5) The distribution of crack lengths at a certain stress and cycles for crack group F_1 can be evaluated by a statistical calculation which takes into account both the crack initiation and growth behaviours of the distributed cracks. In this case, the experimental results could be explained well by the method in which m was taken as constant and C was a probabilistic variable. On the other hand, the results obtained by the calculation method in which correlation between C and m was taken into consideration did not coincide with experimental results.

References

[1] Shiozawa, K., *et al.*, J. Soc. Materials Sci.(in Japanese), 27-293(1978),169.

[2] Shiozawa, K., *et al.*, J. Soc. Materials Sci.(in Japanese), 28-311(1979),745.

[3] Ishihara, S., *et al.*, J. Soc. Materials Sci.(in Japanese), 31-343(1982),390.

[4] Ishihara, S., *et al.*, J. Soc. Materials Sci.(in Japanese), 32-363(1983),1390.

[5] Kitagawa, H., *et al.*, ASTM Spec. Tech. Publ., 642(1978).98.

[6] Kitagawa, H., *et al.*,Proc.Jpn.Soc.Mech. Engrs(in Japanese),No.790-3(1979),254.

[7] Tokaji, K., *et al.*, J. Soc. Materials Sci.(in Japanese), 30-328(1981),15.

[8] Sasaki, S., *et al.*, Proc.Jpn.Soc.Mech. Engrs(in Japanese),No.790-3(1979),251.

[9] Tanaka, T., *et al.*, J. Soc. Materials Sci.(in Japanese), 30-332(1981),83.

[10] Tokaji, K., *et al.*,Preprint of the 31th meeting of the Soc.Materials Sci.(in Japanese),(1982),17.

[11] Kitagawa, H., J. Soc. Materials Sci. (in Japanese), 26-284(1977),489.

[12] Miyata, H. and Kusumoto, S., Trans.Jpn. Soc.Mech.Engrs.(in Japanese), 45-391,A (1979),254.

[13] Sakai, T. and Tanaka, T., J.Soc.Materials Sci.(in Japanese),28-312(1979),880.

[14] Fukuda, S., J, Soc.Materials Sci.(in Japanese), 29-316(1980),9.